Ultrasound in Med. & Biol., Vol. 38, No. 12, pp. 2130–2137, 2012
Published by Elsevier Inc. on behalf of World Federation for Ultrasound in Medicine & Biology

0301-5629/$ - see front matter

http://dx.doi.org/10.1016/j.ultrasmedbio.2012.07.024

● *Original Contribution*

ULTRASONIC ASSESSMENT OF THERMAL THERAPY IN RAT LIVER

JEREMY P. KEMMERER and MICHAEL L. OELZE
Bioacoustics Research Laboratory, Department of Electrical and Computer Engineering, University of Illinois at Urbana-Champaign, Urbana, IL

(*Received* 19 *December* 2011; *revised* 23 *July* 2012; *in final form* 25 *July* 2012)

Abstract—One way to assess the efficacy of thermal therapy is to quantify changes in tissue properties through ultrasonic interrogation, which requires knowledge of the acoustic properties of thermally treated tissues. In this study, estimates of ultrasonic attenuation, speed of sound, backscatter coefficient (BSC), and scattering property estimates were generated from rat liver samples submersed for 10 minutes in a saline bath that was heated to one of seven temperature values over a range of 37–70°C. The attenuation coefficient increased monotonically with exposure temperature, with a maximum increase of 90%. Speed of sound changed by <1% for the different treatment conditions. The BSC had close agreement for all thermal doses over the frequency range of 8–15 MHz. Above this frequency range, samples heated ≥55°C demonstrated an increased BSC slope, and the effective scatterer diameter and effective acoustic concentration were able to distinguish treated from nontreated cases. The findings suggest that attenuation and either BSCs or scatterer property estimates above 15 MHz were sensitive to tissue changes in excised liver caused by thermal therapy. (E-mail: kemmere1@illinois.edu) Published by Elsevier Inc. on behalf of World Federation for Ultrasound in Medicine & Biology.

Key Words: **Quantitative ultrasound, Thermal therapy, Backscatter coefficient, HIFU, Hyperthermia, Sound speed, Attenuation, Ultrasonic tissue properties.**

INTRODUCTION

Ultrasound is intrinsically well-suited to providing fast, safe and affordable diagnostic imaging capabilities to clinicians, and recent developments have demonstrated the potential of ultrasound to yield operator-independent and tissue-specific information. Quantitative ultrasound (QUS) refers to a set of approaches wherein the backscattered ultrasound signal is used to characterize tissue media through model-based parameter estimation. QUS techniques have been demonstrated to be capable of discriminating among several types of animal and human tumors (Lizzi et al. 1997; Oelze and Zachary 2006; Oelze and O'Brien Jr. 2006; Mamou et al. 2011). Lizzi et al. (1997) proposed using QUS techniques for therapy evaluation, and applications of QUS techniques to characterizing radiotherapy (Vlad et al. 2009) and monitoring thermal therapy (Ghoshal et al. 2011) have been examined.

The ultrasonic properties of attenuation, speed of sound and backscatter coefficient (BSC) in soft tissues, and liver specifically, vary with temperature, as has been demonstrated in studies spanning several decades. Goss et al. (1978, 1980) compiled the ultrasonic properties of soft tissues for a range of temperature conditions over which ultrasonic measurements were taken. Other studies considered the issue of the temperature dependency of ultrasonic properties directly. Bamber and Hill (1979) found that above ~40°C, the attenuation coefficient from 1–7 MHz in freshly excised tissues increased with temperature (measured up to 65°C), whereas speed of sound reached a maximum at around 50°C. Damianou et al. (1997) studied the attenuation and absorption in dog liver as a function of temperature and corresponding thermal dose and found that attenuation increased above approximately 50°C or 100 equivalent minutes at 43°C. Gertner et al. (1997) studied the effects of increasing temperature on the attenuation and backscatter of bovine liver from 2.5–5 MHz and found significant increases in attenuation coefficient and small changes in BSC.

Knowledge of the variation of ultrasonic properties in tissues with temperature is critical for developing an ultrasonic technique for monitoring thermal therapy. Likewise, isolating the irreversible effects of thermal exposure from the transient effects of elevated

Address correspondence to: Jeremy Paul Kemmerer, Department of Electrical and Computer Engineering, University of Illinois at Urbana-Champaign, 405 N. Mathews, Urbana, IL 61081. E-mail: kemmere1@illinois.edu

temperature is required to assess thermal therapies in tissues. These permanent effects can be isolated by examining the ultrasonic properties of tissues at a constant subtherapeutic temperature after thermal treatment. Techavipoo et al. (2004) studied propagation speed and attenuation in canine liver tissue over the temperature range 22–90°C and concluded that propagation speed varies only with temperature, with a maximum around 60°C, whereas attenuation varies with both temperature and coagulation effects. Measurements were taken at elevated temperature and at 37°C after exposure, with the latter showing significant increases in attenuation with increasing exposure temperature. Clarke et al. (2003) studied changes in insertion loss measurements with heating for *in vitro* porcine liver from 2–5 MHz and found that attenuation estimates increased significantly (up to 90%). Insertion loss measurements were taken at room temperature, and exposure temperature varied from 40–80°C. Bush et al. (1993) demonstrated that lesions in pig liver generated by an ultrasonic source resulted in measurable changes in acoustic properties. Mechanical effects such as cavitation were suspected by the authors, and the temperature history was unknown, although temperatures up to 95°C were recorded in test samples. Gertner et al. (1998) studied the effects of thermally induced damage in bovine liver *via* heat conduction and microwave heating both during and after thermal exposure through brightness changes in B-mode images. However, these results do not necessarily relate directly to a single ultrasonic property or offer insight into the changes in tissue structure that might produce these observed changes. A better understanding of the changes in ultrasonic properties in regions of thermal damage with respect to these properties in nontreated tissues, as well as an understanding of the changes in tissue structure that are responsible for these changes is required for ultrasonic assessment of thermal therapies and for staging ultrasonic therapy in and around previously exposed regions.

The aim of this study was to estimate changes in ultrasonic BSC, attenuation, and speed of sound of rat liver tissue caused by exposure to different heating regimes, *i.e.*, different thermal doses. As an extension to previous studies in the literature, these properties were estimated from ultrasonic measurements at relatively high frequencies (8 to 25 MHz). To isolate the effects of thermal exposure from temperature-related effects and mechanical sources of damage, the ultrasonic properties of liver tissue were measured at a baseline temperature of 37°C in degassed saline for both thermally treated and nontreated samples, and thermal damage was applied *via* exposure to a degassed saline bath at elevated temperature.

MATERIALS AND METHODS

Sample preparation

The experimental protocol was approved by the Institutional Animal Care and Use Committee of the University of Illinois at Urbana-Champaign and satisfied all university and National Institutes of Health rules for the humane use of laboratory animals. Animals were euthanized through CO_2 according to acceptable procedures as approved by AVMA guidelines on euthanasia of animals. Immediately after euthanasia, the livers were extracted from the rats for experimental use.

Fifty-three liver sections from 16 female Sprague-Dawley rats were examined in this study, wherein a sample constituted a sectioned region of liver tissue treated at a particular temperature. These samples were divided into a low-exposure-temperature (group I) and a high-exposure-temperature group (group II), and each group contained samples from the same animals. Group I was composed of samples exposed to 37, 45, 50 and 55°C, and group II was composed of samples exposed to 37, 60, 65 and 70°C. All exposures were 10 min in duration. Comparisons were made for each sample treated above 37°C with respect to the 37°C (nontreated) sample from the same animal to minimize the effects of biological variation. Liver lobe sections treated at the various temperature levels from each animal were scanned simultaneously (Fig. 1) after treatment to control for any scan-related effects.

During treatment, each liver lobe section was placed in a saline bath at one of the several temperature levels for 10 min. For each animal, at least one lobe section was not treated and was instead placed in a room temperature (20°C) saline bath, whereas the other lobe(s) were being treated in a heated saline bath. These untreated samples are referred to as "37°C exposures" because they were later heated to and maintained at 37°C in the scanning bath. The exposure duration of 10 min was chosen to

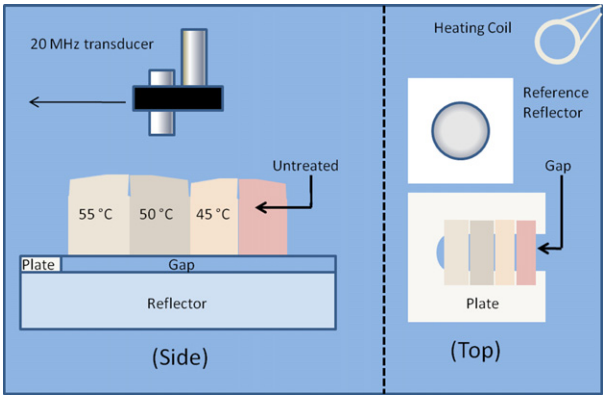

Fig. 1. Experimental setup.

Table 1. Thermal dose corresponding to each treatment temperature

Exposure temperature (°C)	Thermal dose (log_10 min at 43°C)
45	1.5
50	3.0
55	4.5
60	6.0
65	7.5
70	9.0

provide a uniform exposure throughout the sample while keeping the exposure time relatively short. The liver lobe sections were treated in saline for 10 min at 45 ± .5°C, 50 ± .5°C, 55 ± .5°C, 60 ± .5°C, 65 ± .5°C or 70 ± .5°C. It was noted that approximately 2 min was required for the center of each sample to reach within 0.5°C of the bath temperature. Table 1 shows a range of thermal doses for each heating regime. Thermal dose, as defined by Sapareto and Dewey (1984), establishes the equivalent exposure time at 43°C required to produce the effect of a particular exposure time and temperature. The different thermal treatments resulted in distinct coloring of the sample, from a dark red in the unheated case to almost white in the case of the highest temperature exposure. All sections of the liver from a particular animal were affixed to a thin plate above a 1-cm-wide slit using pins, and sample and plate were then placed above a flat reflector plate. Figure 1 depicts the experimental setup, wherein a single scan slice contains regions from each sample section. Immediately after ultrasonic scanning, the samples were placed in 10% neutral buffered formalin, and slides were prepared for histologic examination by staining with hematoxylin and eosin. Excised livers degrade over time and high-frequency backscattered ultrasound is sensitive to cell death processes in liver tissues (Vlad et al. 2005). Therefore, liver samples were heated and backscatter scans were completed within 2 h after euthanasia to minimize the effects of tissue decomposition. Although this did not necessarily prevent tissue degradation over the 2-h time span, treated samples were compared with an untreated (37°C) sample that was extracted from the same liver and had the same duration between extraction and scanning.

Ultrasonic data acquisition

Ultrasonic scans were performed in degassed 0.9% saline at 37°C immediately after thermal treatment. Scans were controlled using a positioning system (Daedal, Inc., Harrisburg, PA, USA) and oriented such that a single scan slice contained a region of each sample section. A single-element 20-MHz transducer (Olympus, f-number of 4) was excited using a pulser-receiver (Panametrics 5900, Olympus NDT, Waltham, MA, USA) and connected to a personal computer *via* a 14-bit A/D card with 250-MHz sampling (Strategic Test UF3, Woburn, MA, USA). The transducer had a −6 dB pulse-echo bandwidth from 9–25 MHz. All radiofrequency scan data consisted of at least 100 time averages. Data acquisition was controlled using custom software (LabView, National Instruments, Austin, TX, USA). Tank temperature was maintained using a heating element and feedback temperature controller (YSI, Yellow Springs, OH, USA).

Backscattered ultrasound and insertion loss measurements were taken in the same lateral region with respect to the sample in a series of parallel 2-D scan slices. Each backscattered ultrasound 2-D scan slice consisted of scan lines spaced 150 μm apart, and five or six slices were taken per scan separated by 1 mm. Scan slices were oriented such that each sample section was contained in every scan slice (Fig. 1). The length of each scan slice was a function of the sample dimensions but typically covered between 20 and 30 mm. The focus was positioned slightly below the center of the sample for backscatter measurements. Insertion loss measurements were performed with a spacing of 1 mm between scans in both lateral directions and with the transducer focus located at the top surface of the reference reflector situated behind the samples. A reference scan for backscatter measurements was performed by recording the reflections from a smooth plate of Plexiglas of known reflectivity. For the reference, waveforms were recorded throughout the transducer depth of field with a spacing of 100 μm. An attenuation reference scan was performed for each sample by repeating the insertion loss scan without the sample in place.

Attenuation and speed of sound estimation

Sample thickness was estimated from backscatter measurements using a speed of sound in 37°C saline of 1533 m/s and three time-of-flight values in the saline. The distance from the transducer to the stationary reflector plate was estimated from the time-of-flight of the transducer reflection at the plate without the liver sample in place. The distance from the transducer to the top of the sample and the distance from the bottom of the sample to the reflector plate with the sample in place were likewise estimated based on the liver-saline interface reflections. The sample thickness was estimated as the difference between the total distance from the transducer to the plate and the sum of the estimated distances in saline with the sample in place. The estimated sample thickness was used to determine the attenuation coefficient *via* a pulse-echo insertion loss measurement. Maximum sample cross-sectional thickness ranged from approximately 5–10 mm, and the samples tapered smoothly to the edges, where the thickness was negligible. Liver sample length was typically around 4 cm, and the width

of the sample was around 1 cm after bisecting the liver in this dimension. The attenuation coefficient with respect to 37°C saline, which is estimated from the log difference of the reflected power spectrum from a reference reflector with and without the sample in place, was computed as the linear slope of the frequency-dependent attenuation, as developed by D'Astous and Foster (1986):

$$\alpha(f) = \alpha_{saline}(f) + \frac{10}{2d}\log_{10}\left(\frac{P_r(f)}{P_s(f)}\right), \quad (1)$$

where $P_r(f)$ is the power spectrum of the windowed scan line from the reference measurement, $P_s(f)$ is the power spectrum of the waveform reflected from the plate with the sample in place and d is the estimated sample thickness as a function of lateral position. The sample speed of sound was estimated by dividing the estimated sample thickness by the time difference between the sample interface reflections.

Backscatter coefficient and parameter estimation

The ultrasonic BSC is a measure of the backscattered energy per unit volume of a material and is related to the underlying structure of tissue. The BSC was determined for each of several nonoverlapping data blocks from the normalized power spectrum:

$$W(f) = \frac{\gamma^2}{4}\frac{1}{|S_0(f)|^2}\frac{1}{N}\sum_l |S_l(f)|^2, \quad (2)$$

where γ is the reflection coefficient of the reference reflector, S_l is the power spectrum estimated from a defined scan line and S_0 is the power spectrum of the reference waveform. A data block is a collection of adjacent windowed radiofrequency segments used in spectral analysis, and the set of data blocks comprise the analysis region of interest (ROI). Attenuation compensation was performed on the normalized power spectrum, and the BSC was estimated using the method of Chen et al. (1997). For each tissue section, the average attenuation coefficient from estimates for the corresponding thermal dose was used for attenuation compensation. In this case, a power law was used to fit the experimental data and obtain an estimate of the frequency-dependent attenuation. Table 2 summarizes the power law fits corresponding to each thermal dose.

Table 2. Power law coefficient attenuation fit

Exposure temperature (°C)	A	n
37	0.138	1.49
45	0.206	1.37
50	0.191	1.44
55	0.233	1.41
60	0.309	1.37
65	0.329	1.38
70	0.342	1.39

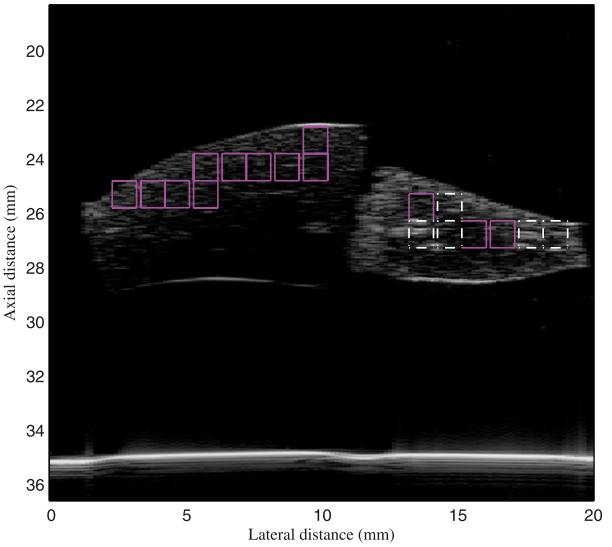

Fig. 2. Block selection. Dashed outline indicates block was excluded because of specular scattering.

QUS parameters of ESD and EAC were estimated from the BSC using the method of Oelze et al. (2002). A spherical Gaussian form factor model was assumed, which represents a scattering particle with a gradual change in impedance compared with the background impedance and has an effective radius related to the fall-off of the impedance distribution. QUS estimates were obtained by choosing a ROI and breaking the ROI into smaller data blocks for analysis. Data blocks from which estimates were computed were selected with respect to their position both within the sample and also with respect to the transducer depth of field. The focus of the imaging transducer was placed several millimeters below the surface of the liver sample, although nonuniform sample

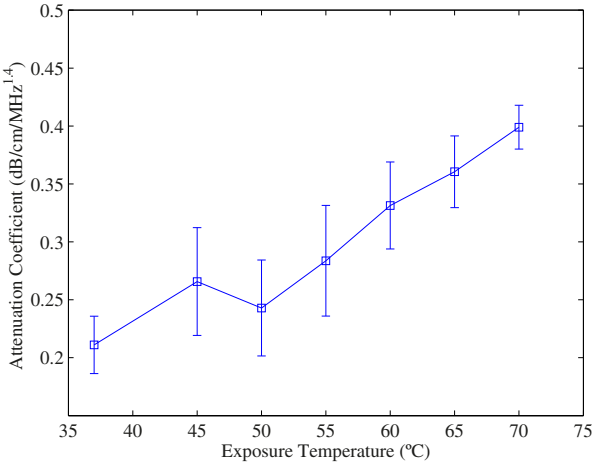

Fig. 3. Attenuation *versus* exposure temperature.

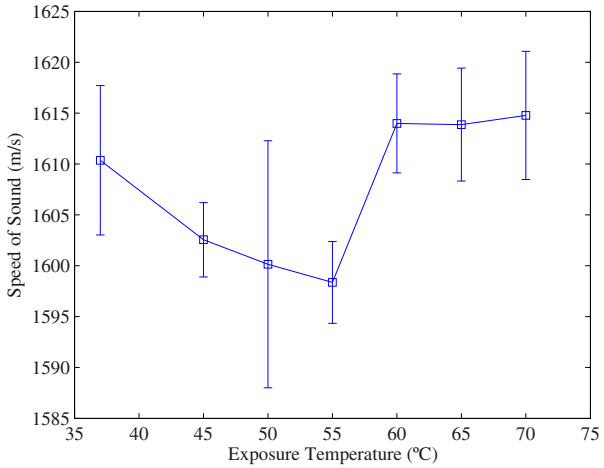

Fig. 4. Speed of sound *versus* exposure temperature.

thicknesses resulted in the focus being located at varying depths in a sample. Data blocks that were sufficiently shallow with respect to the sample interface were considered, resulting in a higher signal-to-noise ratio (SNR). The data blocks had an axial length of 1 mm corresponding to the size of the Hanning window gating the signals and a lateral length of 1 mm corresponding to approximately three beamwidths or six adjacent scan lines.

Because of the structure of liver, larger blood vessels often produced a bright specular reflection in data blocks that contained them and at times produced a shadowing effect, suggesting they might be highly attenuating. For this reason, care was taken to avoid selecting data blocks containing large vessels in both BSC and attenuation estimates. To this end, data blocks were classified according to a threshold in their time-domain signal variance. Data blocks containing an average signal with a variance above an experimentally determined threshold were assumed to contain a specular reflector and excluded from analysis.

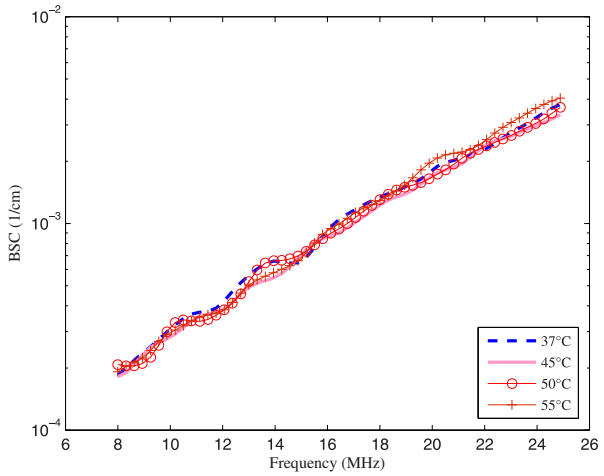

Fig. 5. Average BSC for 37, 45, 50 and 55°C exposures.

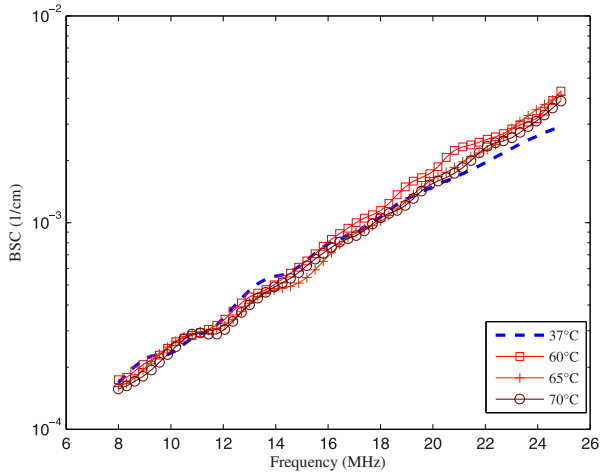

Fig. 6. Average BSC for 37, 60, 65 and 70°C exposures.

Figure 2 shows a sample B-mode image of a scan slice with excluded data blocks indicated.

RESULTS

Attenuation and speed of sound

Estimates of attenuation slope increased monotonically as a function of increasing thermal exposure, as shown in Figure 3. Specifically, the attenuation slope nearly doubled comparing the highest exposure to the baseline, increasing from 0.21 dB/cm/MHz$^{1.4}$ to 0.4 dB/cm/MHz$^{1.4}$. Changes in speed of sound estimates with respect to different exposure regimes were small, changing on average by $<1\%$ compared with the baseline estimate. Figure 4 summarizes the speed of sound estimates. These findings, which describe the speed of sound of treated liver at 37°C after undergoing irreversible changes, are distinct from temperature-dependent properties of liver tissue previously reported.

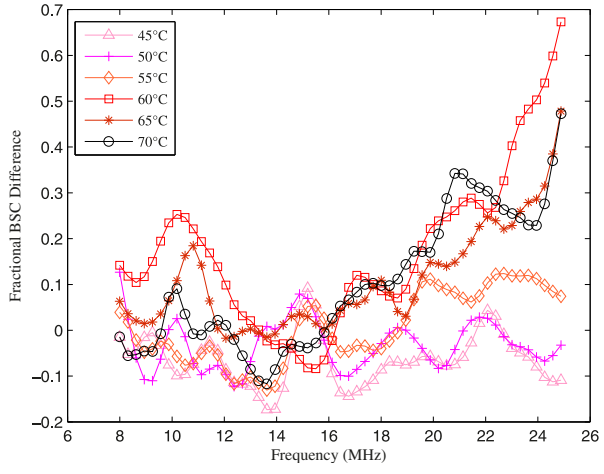

Fig. 7. Fractional difference in average BSC (from nontreated): 45, 50, 55, 60, 65 and 70°C.

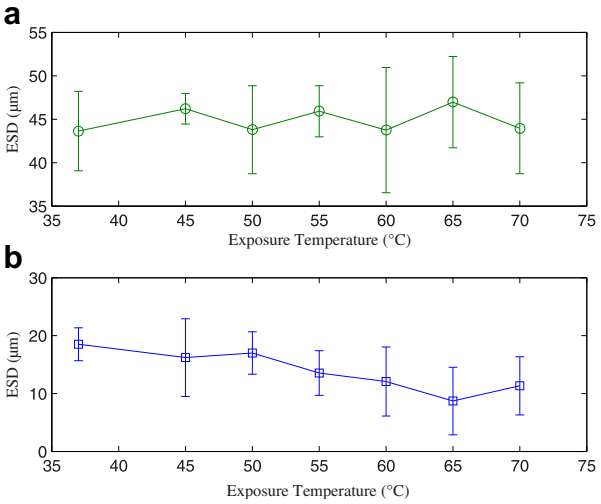

Fig. 8. Average ESD *versus* exposure temperature: (a) 8–15 MHz, (b) 15–25 MHz.

Backscatter

Figures 5 and 6 show the average of BSCs from all included data blocks for each thermal dose over the frequency bandwidth of the transducer (8 to 25 MHz). Estimates of BSC were observed to have two distinct trends over two different intervals of the frequency ranges examined. From 8–15 MHz, the average BSCs were nearly identical over all heating regimes. From 15–25 MHz, however, an increasing trend in BSC for thermal doses corresponding to the 55°C exposure and above were observed compared with lower thermal doses and nontreated samples. The BSCs from exposures corresponding to <55°C were observed to closely match over the entire bandwidth examined. Figure 7 shows the fractional difference in the average BSC of each thermal dose compared with the average nontreated BSC. Each average BSC for treated samples was compared with the corresponding average nontreated BSC for liver from the same animals. Above 15 MHz, the 55, 60, 65 and 70°C exposures had an increasing fractional difference with frequency, whereas the 45 and 50°C exposures had a fractional difference that was nearly constant with frequency. Statistical significance of the changes in BSC with thermal therapy was assessed by fitting a model to the average BSC curves and comparing the resulting parameters.

To parameterize the BSC, a spherical Gaussian scattering model was fit to the average BSC estimate for each sample, and the ESD and EAC were obtained. Figure 8a and 8b shows average ESD estimates *versus* exposure temperature for parametric fits to the BSC data for 8- to 15-MHz and 15- to 25-MHz frequency ranges, respectively. Although no apparent separation appears for parametric fits from 8–15 MHz, ESD parameters derived from the 15- to 25-MHz data demonstrated a decreasing trend with increasing thermal dose. One-way analysis of variance revealed statistically significant differences ($p < 0.05$) in ESD estimates for 60, 65 and 70°C exposures for the 15- to 25-MHz frequency range compared with the corresponding 37°C exposures estimates. No statistically significant differences in ESD were observed for the remaining exposure conditions, including all 8- to 15-MHz frequency range ESD estimates. ESD and EAC parameters for all thermal doses and both frequency ranges are summarized in Table 3. The ESD and EAC were observed to change appreciably with respect to the nontreated cases in the 15- to 25-MHz frequency range, but not in the 8- to 15-MHz frequency range. The two average values for the nontreated (37°C) exposure correspond to groups I and II as indicated.

Histology

Histology slides of sample sections from liver samples treated at each thermal dose were examined by a pathologist, and two effects as a function of increasing thermal dose were noted. First, cellular damage to blood vessels and the cells at the tissue surface were extensive and increased with exposure temperature. Second, the samples with exposure >55°C appeared to show a progression of dilated sinusoids. Figures 9–11 show digitized histology slides at 40x magnification for the nontreated, 55°C and 70°C exposures, respectively. The images show hepatocytes surrounding a central vein, with sinusoids appearing progressively more dilated with increasing treatment exposure temperature.

Table 3. ESD and EAC from mean BSC for each thermal dose

Exposure temperature (°C)	ESD (μm) (8–15 MHz)	EAC (dB) (8–15 MHz)	ESD (μm) (15–25 MHz)	EAC (dB) (15–25 MHz)
37	44.8(I), 44.3(II)	31.4(I), 31.09(II)	17.8(I), 18.8(II)	50.6(I), 48.6(II)
45	46.3	31.0	17.8	50.3
50	43.5	32.3	17.8	50.4
55	46.0	31.2	14.5	55.4
60	46.0	30.6	11.75	60.1
65	47.8	29.8	5.0	81.3
70	45.0	30.7	11.0	61.2

Results from each group are denoted with (I) and (II).

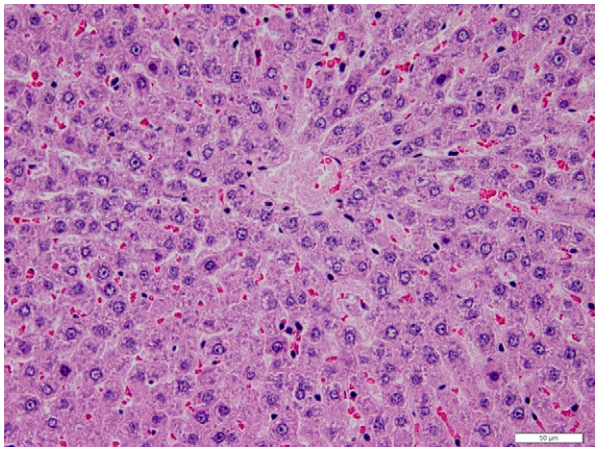

Fig. 9. Digitized histology slide image of nontreated liver tissue.

DISCUSSION

The results of this study have important implications for ultrasonic assessment of thermal injury to liver. First, attenuation demonstrated the highest sensitivity to the degree of thermal dose given to liver samples examined in this study. The attenuation coefficient increased monotonically with increasing thermal dose and changed by up to 90%. This trend of increasing attenuation with heating was also noted by several authors (Bush et al. 1993; Gertner et al. 1997; Clarke et al. 2003) at lower frequencies. These increases have been attributed to protein denaturation resulting from elevated temperature, an idea consistent with earlier findings that absorption in soft tissues is related to protein content (Goss et al. 1979). Speed of sound estimate changes were small and did not change monotonically with exposure temperature, which is consistent with the findings of Techavipoo et al. (2004). BSC changes with respect to the nontreated baseline appeared at and above the thermal doses corresponding to 55°C exposure in the 15- to 25-MHz frequency range. BSC estimates from 8–15 MHz matched closely for all exposure regimes. This finding agrees with findings of other studies of BSC changes with heating at lower frequencies (Bush et al. 1993; Gertner et al. 1997), which observed that changes in BSC in liver caused by thermal exposure were small. As a result, separation of unheated and heated sample QUS estimates occurred only in the 15- to 25-MHz frequency range.

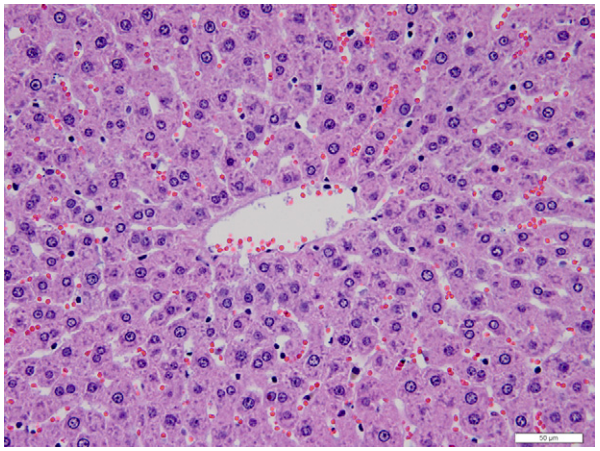

Fig. 10. Digitized histology slide image of 55°C treated liver tissue.

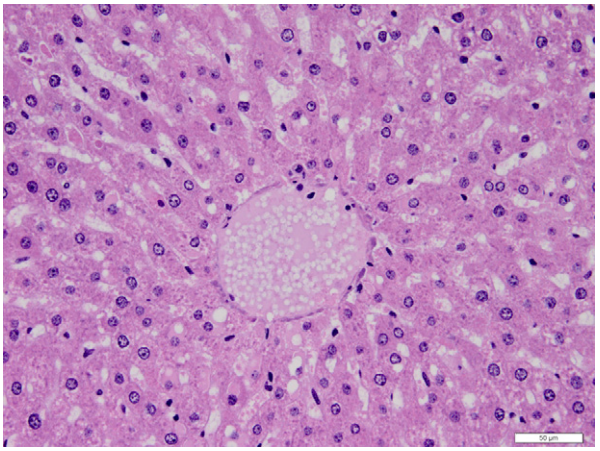

Fig. 11. Digitized histology slide image of 70°C treated liver tissue.

The differences in heated and unheated BSCs >55°C and 15 MHz suggest that the sensitivity of backscatter-based QUS techniques may be caused by changes at the cellular level. For 15 MHz and above, scatterer sizes such that $ka = 1$ correspond to diameters <33 μm. From histology images, liver cell sizes were in the range of 20–25 μm, whereas the cell nuclei were approximately 10 μm. These results, combined with the observation that increasing exposure dose resulted in sinusoidal dilation and a smaller ESD, may indicate that the ESD is related to intercellular spacing. Another possibility is that BSC differences are related to changes in the nucleus of the cell as a result of heating ($ka = 0.4$ for a 10-μm nucleus diameter at 20 MHz), which may result in nuclear condensation.

The issue of relating BSC estimates to histology and the effects of heating are complicated by cell death and fixation processes. Because liver tissue is very metabolically active, the cellular changes responsible for differences in heated and unheated BSC estimates may result from the interaction of tissue heating and decay as the result of extraction (ischemia), which would not occur *in vivo*. Also, the time required after the BSC measurements for insertion loss scans and tissue fixation for each sample, as well as the fixation process itself, could have resulted in differences between tissue morphology in the slides and during the scans, potentially masking

any measured changes induced by heating. Demonstrating similar changes in *in vivo* liver samples and studying treated liver samples that have been fixed immediately after heating could clarify these findings.

CONCLUSION

The close agreement in BSCs across heating regimes at frequencies between 8 and 15 MHz, which most closely coincide with the bandwidth that is currently achievable on clinical devices, suggests that backscatter-based QUS parameters may be relatively insensitive to thermal injury in liver in the clinical frequency range. However, if the BSC is constant over thermal dose, it may be possible to use this information to extract other ultrasonic properties from backscatter (*e.g.*, attenuation). Estimating degree of thermal exposure from a spatial map of attenuation, which increased monotonically with thermal exposure temperature, may be the most promising approach to assessing thermal therapy in liver tissue using ultrasound. However, although these results may hold for normal liver tissues, it is still necessary to conduct similar studies for other tissues, such as tumors, which may yield distinctly different property changes with thermal treatment.

Acknowledgments—The authors would like to acknowledge the technical assistance of Dr. Rita Miller, Dr. Goutam Ghoshal, Dr. Sandhya Sarwate and Tiantian Tang.—The work was supported by NIH Grant R01 EB008992 (National Institutes of Health, Bethesda, MD).

REFERENCES

Bamber JC, Hill CR. Ultrasonic attenuation and propagation speed in mammalian tissues as a function of temperature. Ultrasound Med Biol 1979;5:149–157.

Bush NL, Rivens I, ter Haar GR, Bamber JC. Acoustic properties of lesions generated with an ultrasound therapy system. Ultrasound Med Biol 1993;19:789–801.

Chen X, Phillips D, Schwarz KQ, Mottley JG, Parker KJ. The measurement of backscatter coefficient from a broadband pulse-echo system: a new formulation. IEEE Trans Ultrason Ferroelectr Freq Control 1997;44:515–525.

Clarke RL, Bush NL, ter Haar GR. The changes in acoustic attenuation due to *in vitro* heating. Ultrasound Med Biol 2003;29:127–135.

D'Astous FT, Foster FS. Frequency dependence of ultrasound attenuation and backscatter in breast tissue. Ultrasound Med Biol 1986; 12:795–808.

Damianou CA, Sanghvi NT, Fry FJ, Maass-Moreno R. Dependence of ultrasonic attenuation and absorption in dog soft tissues on temperature and thermal dose. J Acoust Soc Am 1997;201:628–634.

Gertner MR, Wilson BC, Sherar MD. Ultrasound properties of liver tissue during heating. Ultrasound Med Biol 1997;23: 1395–1403.

Gertner MR, Worthington AE, Wilson BC, Sherar MD. Ultrasound imaging of thermal therapy in in vitro liver. Ultrasound Med Biol 1998;24:1023–1032.

Ghoshal G, Luchies A, Blue JP, Oelze ML. Temperature dependent ultrasonic characterization of biological media. J Acoust Soc Am 2011;130:2203–2211.

Goss SA, Frizzell LA, Dunn F, Dines KA. Dependence of the ultrasonic properties of biological tissue of constituent proteins. J Acoust Soc Am 1979;67:1041–1044.

Goss SA, Johnston RL, Dunn F. Comprehensive compilation of empirical ultrasonic properties of mammalian tissues. J Acoust Soc Am 1978;64:423–457.

Goss SA, Johnston RL, Dunn F. Compilation of empirical ultrasonic properties of mammalian tissues II. J Acoust Soc Am 1980;68: 93–108.

Lizzi FL, Astor M, Liu T, Deng C, Coleman DJ, Silverman RH. Ultrasonic spectrum analysis for tissue assays and therapy evaluation. Int J Imaging Syst Technol 1997;8:3–10.

Mamou J, Coron A, Hata M, Machi J, Yanagihara E, Laugier P, Feleppa EJ. Three-dimensional high-frequency characterization of cancerous lymph nodes. Ultrasound Med Biol 2010;36:361–375.

Oelze ML, O'Brien WD Jr. Application of three scattering models to the characterization of solid tumors in mice. Ultrason Imaging 2006;28: 83–96.

Oelze ML, Zachary JF. Examination of cancer in mouse models using quantitative ultrasound. Ultrasound Med Biol 2006;32: 1639–1648.

Oelze ML, Zachary JF, O′Brien WD Jr. Characterization of tissue microstructure using ultrasonic backscatter: theory and technique for optimization using a Gaussian form factor. J Acoust Soc Am 2002;112: 1202–1211.

Sapareto SA, Dewey WC. Thermal dose determination in cancer therapy. Int J Radiat Oncol Biol Phys 1984;10:787–800.

Techavipoo U, Varghese T, Chen Q, Stiles TA, Zagzebski JA, Frank GR. Temperature dependence of ultrasonic propagation speed and attenuation in excised canine liver tissue measured using transmitted and reflected pulses. J Acoust Soc Am 2004;115:2859–2865.

Vlad RM, Czarnota GJ, Giles A, Sherar MD, Hunt HW, Kolios MC. High-frequency ultrasound for monitoring changes in liver tissue during preservation. Phys Med Biol 2005;50:197–213.

Vlad RM, Brand S, Giles A, Kolios MC, Czarnota GJ. Quantitative ultrasound characterization of responses to radiotherapy in cancer mouse models. Clin Cancer Res 2009;15:2067–2075.